

The catecholaminergic innervation of the claustrum of the pig

Andrea Pirone,¹  Vincenzo Miragliotta,¹  Federica Ciregia,^{2,3}  Elisabetta Giannessi¹  and Bruno Cozzi⁴ 

¹Department of Veterinary Sciences, University of Pisa, Pisa, Italy

²Department of Clinical and Experimental Medicine, University of Pisa, Pisa, Italy

³Department of Pharmacy, University of Pisa, Pisa, Italy

⁴Department of Comparative Biomedicine and Food Science, University of Padova, Legnaro, PD, Italy

Abstract

Over the past decades, the number of studies employing the pig brain as a model for neurochemical studies has dramatically increased. The key translational features of the pig brain are the similarities with the cortical and subcortical structures of the human brain. In addition, the caudalmost part of the pig claustrum (CL) is characterized by a wide enlargement called posterior puddle, an ideal structure for physiological recordings. Several hypotheses have been proposed for CL function, the key factor being its reciprocal connectivity with most areas of the cerebral cortex and selected subcortical structures. However, afferents from the brainstem could also be involved. The brainstem is the main source of catecholaminergic axons that play an important neuromodulatory action in different brain functions. To study a possible role of the CL in catecholaminergic pathways, we analyzed the presence and the distribution of afferents immunostained with antibodies against tyrosine hydroxylase (TH) and dopamine beta-hydroxylase (DBH) in the pig CL. Here we show that the CL contains significant TH immunoreactive axons contacting perikarya, whereas projections staining for DBH are very scarce. Our findings hint at the possibility that brainstem catecholaminergic afferents project to the CL, suggesting (i) a possible role of this nucleus in functions controlled by brainstem structures; and, consequently, (ii) its potential involvement in the pathophysiology of neurodegenerative pathologies, including Parkinson's disease (PD).

Key words: catecholamine; claustrum; dopamine beta-hydroxylase; immunohistochemistry; pig; tyrosine hydroxylase.

Introduction

Over the past decades, the number of studies employing the pig brain as a model for neurochemical studies has dramatically increased. The key translational features of the pig brain are its size (large enough to allow a wide range of physiological, neurosurgical and imaging investigations) and the similarities with the cortical and subcortical structures of the human brain (Jelsing et al. 2006; Lind et al. 2007). Furthermore, the caudalmost part of the pig CL is characterized by a wide enlargement called posterior puddle (Fig. 1). This latter vast posterior puddle (see Félix et al. 1999; coronal sections A 3.50. to A 0.50) is ideally suited for

physiological recording, which would be difficult to perform in other species because of the small size of the structure and its continuity with adjoining structures (Johnson et al. 2014).

The CL is a subcortical nucleus present in all mammalian species examined so far, including man (Kowiański et al. 1999). The structure, function and origin of the CL are still a matter of debate (Edelstein & Denaro, 2004; Crick & Koch, 2005; Pirone et al. 2012; Mathur, 2014; Deutch & Mathur, 2015; Goll et al. 2015). Recent studies employing innovative techniques have investigated the structural connectivity of the CL (Day-Brown et al. 2016; Reser et al. 2016; Wang et al. 2016; Watson et al. 2016), revealing extensive and reciprocal links with different cortical and subcortical structures. Several articles have described the neurochemistry of the CL, contributing to the understanding of its intrinsic and extrinsic connectivity (Rahman & Baizer, 2007; Kowiański et al. 2009; Cozzi et al. 2014; Hinova-Palova et al. 2014; Pirone et al. 2014, 2015, 2016; Orman et al. 2016). Recently, Barbier et al. (2016) analyzed the

Correspondence

Andrea Pirone, Department of Veterinary Sciences, University of Pisa, Pisa 56124, Italy. E: andrea.pirone@unipi.it

A.P. and V.M. contributed equally to the work.

Accepted for publication 18 August 2017

Article published online 1 October 2017



Fig. 1 Posterior puddle. Photographs of a coronal section of the pig brain showing the caudal part of the claustrum (black circle) that form a large mass of about 0.5 cm in diameter. Scale bar = 1 cm.

innervation of the rat CL, and they did not report the presence of tyrosine hydroxylase (TH)-positive axons. TH is involved in the first, rate-limiting step of catecholamine biosynthesis, hydroxylating the amino acid precursor tyrosine to dihydroxyphenylalanine (L-DOPA), which subsequently is converted into dopamine. The latter, by means of dopamine- β -hydroxylase (DBH), is transformed into norepinephrine (Craine & Daniels, 1973; Daubner et al. 2012).

TH-immunoreactive axons represent dopaminergic and noradrenergic afferents from the ventral tegmental area (VTA) and the locus coeruleus, respectively (Chandler, 2016; Morales & Margolis, 2017). Dopaminergic neurons are also localized in the substantia nigra, pars compacta, and their projections to the dorsal striatum give rise to the nigrostriatal pathway. Degeneration of these neurons is linked directly to symptoms of Parkinson's disease (PD) (Brichta et al. 2013; Ledonne & Mercuri, 2017). Within this relatively well known framework, some studies performed in the last decade have hypothesized a specific role for the CL, including acting as 'orchestra conductor' (Crick & Koch, 2005); sensory integration/coincidence detection (Smythies et al. 2014); modulation/switching of cortical functional networks (Reser et al. 2014); modulation of selective attention (Mathur, 2014); and a center for delusional states (Patru & Reser, 2015). These hypotheses are grounded on the reciprocal connectivity of the CL with most areas of the cerebral cortex and with selected subcortical structures. However, brainstem afferents could also be involved; in particular, dopaminergic innervation potentially modulate all the functions that have been proposed for the CL.

Considering the scarcity of data on the expression of TH and DBH in the CL, its changes in patients with PD (Braak et al. 2001, 2007; Kalaitzakis & Pearce, 2009) and the relevant neuromodulatory actions of the dopaminergic and noradrenergic systems in the brain, we decided to study the presence of TH and DBH within the pig CL.

Material and methods

Animals and tissue sampling

The brains of 10 adult pigs (*Sus scrofa domesticus*) were removed immediately after commercial slaughtering at a local abattoir (Desideri Luciano SPA, Via Abruzzi, 2 56025 - Pontedera PI, Toscana - Italy). Animals were treated according to the European Regulation (CE1099/2009) concerning animal welfare during the commercial slaughtering process, and were constantly monitored under mandatory official veterinary medical care. All the animals were in good body condition and considered free of pathologies by the veterinary medical officer responsible for the health and hygiene of the slaughterhouse. The brains, extracted within 15 min of death, were cut into transverse sections (0.5 cm thick) containing the CL and the adjoining structures (putamen and insular cortex) in their rostro-caudal extent. Five brains were processed for immunohistochemistry and five for Western blot analysis. Sections were fixed by immersion in 4% paraformaldehyde in 0.1 M phosphate-buffered saline (PBS) at pH 7.4. Tissues from the right hemisphere were processed for paraffin embedding and samples from the left hemisphere after fixation were cryoprotected by saturation in a 20% sucrose solution (Sigma, St. Louis, MO, USA) in 0.1 M phosphate-buffered saline (PBS) for 24 h at 4°C, snap-frozen on powdered dry ice, and stored at -80°C until use.

Western blot

After brain extraction, transverse sections (0.5 cm thick) containing the CL and the adjoining structures were cut. For CL sampling, we considered only the caudal sections because in this region the pig CL presents an exceptional wide extension (Fig. 1). CL, putamen and insula were quickly sampled under a stereomicroscope and immediately stored at -80°C . Protein extracts obtained from porcine CL, insula and putamen were analyzed by Western blot to evaluate the presence of TH and DBH using specific antibodies (Table 1). Aliquots of 30 μg of proteins were resolved by 12% SDS-PAGE gels and transferred onto nitrocellulose membranes (0.2 μm) using a voltage of 25 V for 7 min (Trans-Blot[®]TurboTM Transfer System; Bio-Rad). Membranes were blocked and then incubated appropriately with the following primary antibodies: anti-TH (1 : 300, S. Cruz Biotech., Inc., sc-14007); anti-DBH (1 : 300, Chemicon Int., MAB308). HRP-conjugated goat anti-rabbit (1 : 10 000, Enzo life science, ADI-SAB-300J) and HRP-conjugated goat anti-mouse (1 : 10 000, Perkin Elmer, NEF822) were used as secondary antibodies (Table 2). The chemiluminescent images were acquired by LAS 4010 (GE Health Care).

Immunohistochemistry

Immunoperoxidase reaction was performed on serial paraffin sections (5 μm) using a rabbit polyclonal anti-TH antibody (1 : 300, S. Cruz Biotech., Inc., sc-14007) and a mouse monoclonal anti-DBH

(1 : 300, Chemicon Int., MAB308) (for details regarding the antibodies used, see Tables 1 and 2). Epitope retrieval was carried out at 120 °C in a pressure cooker for 5 min with a Tris/EDTA buffer, pH 9.0. Sections were pretreated with 1% H₂O₂ (in 0.1 M PBS, pH 7.4, 10 min) to quench endogenous peroxidase activity, then rinsed with 0.05% Triton-X (TX) -100 (in 0.1 M PBS, 3 × 10 min), and blocked for 1 h with 5% normal horse serum (PK-7200, Vector Labs, Burlingame, CA, USA) (in 0.1 M PBS). Sections were incubated overnight at 4 °C in a solution containing either the rabbit anti-TH or the mouse anti-DBH with 2% normal horse serum, 0.05% TX-100 (in 0.1 M PBS). Sections were then rinsed in 0.1 M PBS, (3 × 10 min), followed by incubation with either a biotinylated anti-rabbit IgG (5 µg mL⁻¹, BA-1100, Vector Labs) or biotinylated anti-mouse IgG (5 µg mL⁻¹, BA-2001, Vector Labs) and then with ABC reagent (Vectastain Kit, PK-7200, Vector Labs). Sections were again rinsed in 0.1 M PBS for 3 × 10 min. Staining was visualized by incubating the sections in diaminobenzidine (sk-4105, Vector Labs) solution. The specificity of immunohistochemical staining was tested by replacing the primary antibodies, anti-rabbit/mouse IgG or the ABC complex with PBS or non-immune serum. Under these conditions, staining was abolished. Specificity of the DBH antibody had already been tested in previous studies (http://antibodyregistry.org/search.php?q=AB_2314290). Furthermore, we verified the labeling quality of the primary antibodies using cryostat sections of archival rat brains and either cryostat or paraffin sections of the pig brainstem as positive controls. Under these conditions, both antibodies labeled neurons in the locus coeruleus (Supporting Information Figs S1–S3).

Double immunofluorescence

Immunofluorescent reactions were performed on cryostat sections (20 µm) collected on gelatin-coated slides, using a rabbit polyclonal anti-TH antibody (1 : 300, S. Cruz Biotech., Inc., sc-14007), and a mouse monoclonal anti-DBH (1 : 300, Chemicon Int., MAB308), and a mouse anti-neuronal nuclei (NeuN) monoclonal antibody (1 : 1000, MAB377, Millipore). Sections were blocked for 1 h with 2% bovine serum albumin (BSA, A7906, Sigma-Aldrich), 0.1% TX-100 in PBS followed by overnight incubation at 4 °C in a solution containing the rabbit anti-TH and the mouse anti-NeuN (TH/NeuN) with 0.1% BSA, 0.05% TX-100 in PBS. Sections were then rinsed in 0.1 M PBS, (3 × 10 min), and incubated with a fluorescein anti-rabbit IgG (10 µg mL⁻¹, FI-1000, Vector Labs) and Dylight 649 anti-mouse IgG (10 µg mL⁻¹, DI-2649, Vector Labs) for 1 h at room temperature. For DBH/NeuN, double-stained sections were first incubated overnight at 4 °C with DBH, followed by incubation with fluorescein-conjugated anti-mouse IgG (10 µg mL⁻¹, FI-2000, Vector Labs) for 1 h at room temperature. Then, after the first staining, sections were washed with PBS and incubated with NeuN overnight at 4 °C. Tissues were then incubated with anti-mouse IgG (10 µg mL⁻¹, FI-2000, Vector Labs) diluted in PBS for 1 h at room temperature.

Finally, sections were washed with PBS and coverslipped with Vectashield with DAPI (H-1500, Vector Labs).

Image acquisition and processing

Microphotographs were collected under a Nikon Ni-e light microscope (Nikon Instruments Spa Calenzano, Florence, Italy), fully equipped for fluorescence acquisition, connected to a personal computer via Nikon digital image processing software (DIGITAL SIGHT DS-U1, NIS-ELEMENTS BR-4.13.00 software). To better localize the CL

boundaries, selected sections were stained with the Luxol Fast Blue method. The CL and adjoining structures, as well as the boundaries of other key structures examined in the present study, were identified according to a stereotaxic atlas (Félix et al. 1999) using the following coordinates for coronal sections: CL, A 17.50 to A 0.50; *locus coeruleus*, P 5.00–P 9.00; *substantia nigra (pars compacta and pars reticulata)*, A 6.50 to A 1.00; putamen A 17.50 to A 1.50.

Results

Western blot

Immunoblot analysis was performed to evaluate the presence and the expression levels of TH and DBH in the CL, putamen and insula, and to test the specificity of the commercial antibodies selected. A single immunoreactive band at 60 kDa was detected for anti-TH, and two main immunoreactive bands for anti-DBH. All sampled regions were immunoreactive for both TH and DBH; however, TH immunoreactivity was more intense in protein extracts from the putamen than from the CL and especially from the insula (Fig. 2).

Immunohistochemistry

Immunoperoxidase staining revealed that the TH-positive innervation was extremely intense in the putamen, intense in the CL and moderate in the insular cortex (Figs 3 and 4). The anti-TH antibody never labeled either neuronal or neuroglia cell bodies; however, fibers stained positively. Some longitudinal fibers were thicker, dark-stained with spherical varicosities (Fig. 4D). Blood vessel endothelial cells also displayed TH staining (Fig. 5). TH-positive axons running in all directions were seen throughout the rostro-caudal and the dorso-ventral extent of the CL with a homogeneous distribution. There were also many immunostained puncta, possibly the results of cross-sections of fibers running in an anterior-posterior direction. Positive fibers showed numerous varicosities and terminals that surrounded and defined the cell bodies (Fig. 5C,D).

Table 1 Primary antibodies.

Antibody	Immunogen	Manufacturing details	Dilution
Anti-TH	Amino acids 1–196 of TH of human origin	Santa Cruz Biotechnology, rabbit polyclonal, sc-14007	1 : 300
Anti-DBH	Purified bovine DBH	Chemicon International, mouse monoclonal, MAB308	1 : 300
Anti-NeuN	Purified cell nuclei from mouse brain	Millipore, mouse monoclonal, MAB377, A60	1 : 1000

We did not observe any DBH immunoreactivity in paraffin sections, whereas a few axons were found in the CL in the cryostat sections stained with immunofluorescence; the endothelial cells of vessels contained DBH (Fig. 6).

Double immunofluorescence

Observation of sections labeled with a dual immunofluorescence procedure showed that TH axons were in close contact with CL neurons, marked with NeuN (Fig. 5A,B). On the contrary, none of the few DBH fibers seemed to reach cell bodies (Fig. 6).

Discussion

The present study describes the dopaminergic and noradrenergic innervation in the CL of the pig, using TH and DBH, respectively, as immunohistochemical markers. The specificity of the primary antibodies employed was tested by performing a Western blot analysis, which revealed the presence of both TH and DBH in the putamen, in the CL, and in the insula cortex. Two main immunoreactive bands were observed for anti-DBH that probably represent the glycosylated (higher MW) and soluble (lower MW) forms of DBH (Feng et al. 1992). Moreover, the quality of the TH

labeling was supported by the extremely dense immunostaining in the putamen. Immunoperoxidase on paraffin sections did not reveal positivity to DBH in the CL, but in the locus coeruleus (LC) of the pig, DBH-positive neurons were detected (Fig. S3). Moreover, using cryostat sections, very few DBH immunofluorescent fibers were seen in the CL. All the above-mentioned findings led us to speculate that the very low levels of DBH in the CL were not detectable in paraffin-embedded samples: it is indeed known that formalin-fixation-paraffin-embedding commonly results in a decrease in antigenicity. However, we cannot exclude differences between the right and left hemispheres: indeed, the right and left CL may have a slightly different functional significance (Naghavi et al. 2007) and an asymmetrical size (Cao et al. 2003).

We found that both enzymes were expressed by endothelial cells: a former study showed that they are able to synthesize and release catecholamine (Sorriento et al. 2012). The very scarce number of DBH-immunoreactive fibers together with the finding that they were not in contact with perikarya indicate that the CL, at least in this species, is not the target of noradrenergic axons. On the contrary, the presence of an intense TH innervation with positive axons contacting neurons, shows that the CL is a probable recipient for afferents containing dopamine (Fig. 7). This latter

Table 2 Secondary antibodies.

Antibody	Type	Manufacturing details	Dilution
Biotinylated	Anti-mouse IgG (H + L)	Vector Labs, Burlingame, horse, Cat.n. BA-2001, Lot.n. ZC1230	5 $\mu\text{g mL}^{-1}$
Biotinylated	Anti-rabbit IgG (H + L)	Vector Labs, Burlingame, horse, Cat.n. BA-1100, Lot.n. ZA0319	5 $\mu\text{g mL}^{-1}$
Florescein	Anti-rabbit IgG (H + L)	Vector Labs, Burlingame, goat, Cat.n. FI-1000, Lot.n. W1018	10 $\mu\text{g mL}^{-1}$
DyLight 649	Anti-mouse IgG (H + L)	Vector Labs, Burlingame, horse, Cat.n. DI-2649, Lot.n. ZA0424	10 $\mu\text{g mL}^{-1}$
HRP conjugate	Anti-rabbit IgG	Enzo life science, goat, Cat.n. ADI-SAB-300J	1 : 10 000
HRP conjugate	Anti-mouse IgG	Perkin Elmer, goat, Cat.n. NEF822	1 : 10 000

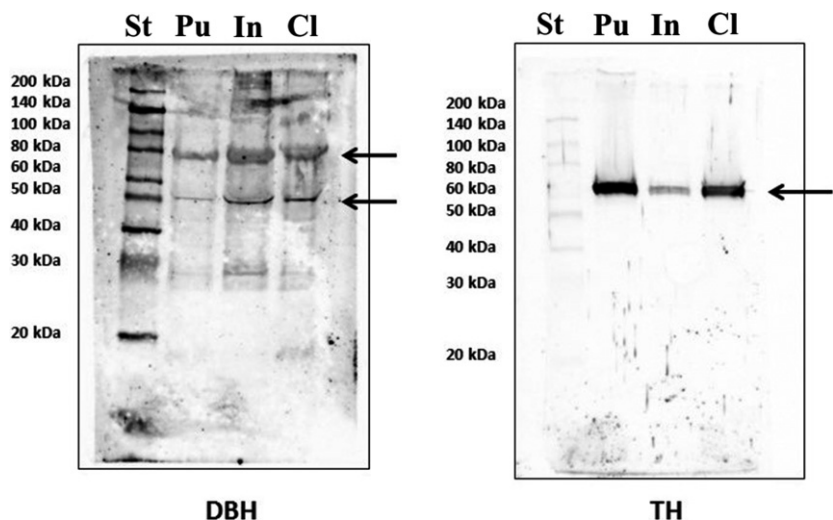


Fig. 2 Western Blot. Immunoblot analysis revealed the presence and the expression levels of both TH and DBH in the putamen (Pu), Insula (In) and claustrum (Cl). A single immunoreactive band at 60 kDa was detected for anti-TH (arrow), while two main immunoreactive bands (arrows) were observed for anti-DBH, probably representing the glycosylated (higher MW) and soluble (lower MW) forms of DBH. St, standard.

hypothesis is further supported by the presence of numerous TH-labeled varicosities which are evidence of the presence of *en passant* synapses.

Former studies corroborate our data, since different dopamine receptor subtypes have been demonstrated in the CL of several species (Cortimiglia et al. 1982; Fuxe et al.

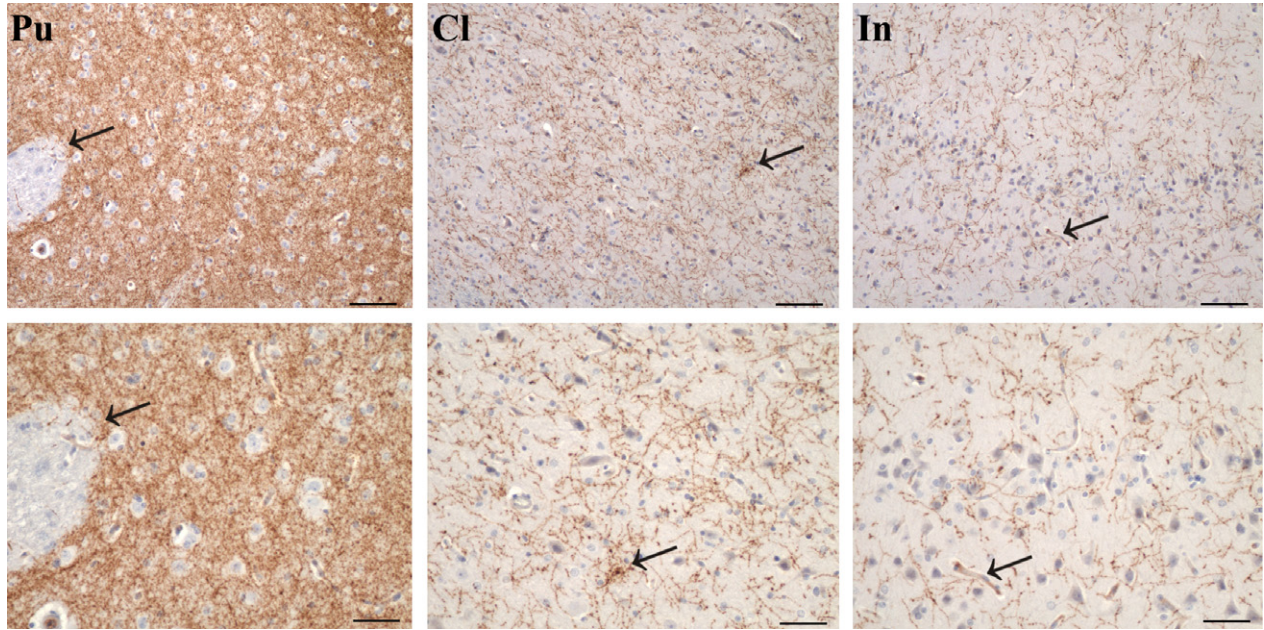


Fig. 3 TH immunohistochemistry. TH-immunoreactive fibers in the putamen (Pu), claustrum (Cl) and insula cortex (In). The immunostaining was extremely dense in the Pu, dense in the Cl and moderate in the In. Arrows indicate the magnified zones. Scale bars in the upper row = 100 μ m, in the lower row = 50 μ m.

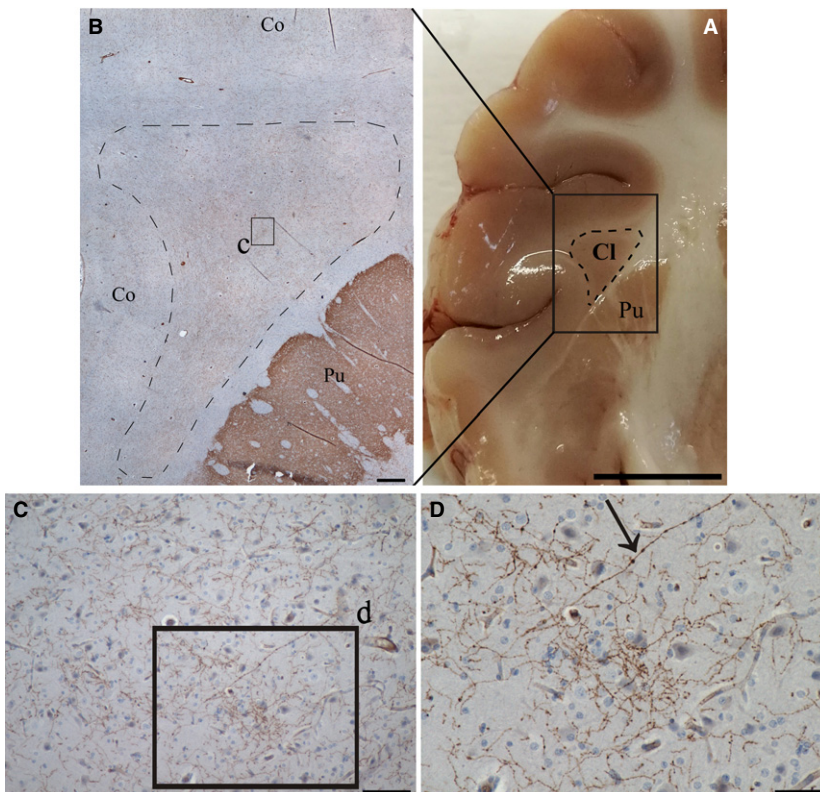


Fig. 4 TH-labeled fibers in the claustrum and adjacent structures. (A) photograph of a coronal section of the pig brain, black rectangle shows the immunostained area represented in figure B. (B) Low magnification image showing immunostaining in the putamen (Pu), in the claustrum (dashed line, Cl) and cortex (Co). (C) Higher magnification of the zone indicated with the black square (c) in image B. (D) Higher magnification of a part (d, black square) of image C, arrow indicates a thick TH fiber with round varicosities. Scale bars = 500 μ m (A), 100 μ m (B), 50 μ m (C), 1 cm (D).

1987; Schiffmann et al. 1990; Meador-Woodruff et al. 1992).

In the literature, data regarding the TH and DBH innervation of the CL are very scarce. Previous studies reported a

faint dopaminergic innervation in the rat CL and a high TH immunostaining in the human CL (Fallon et al. 1978; Sutoo et al. 1994). In a recent study of the rat CL, the authors described melanin-concentrating hormone-positive axons,

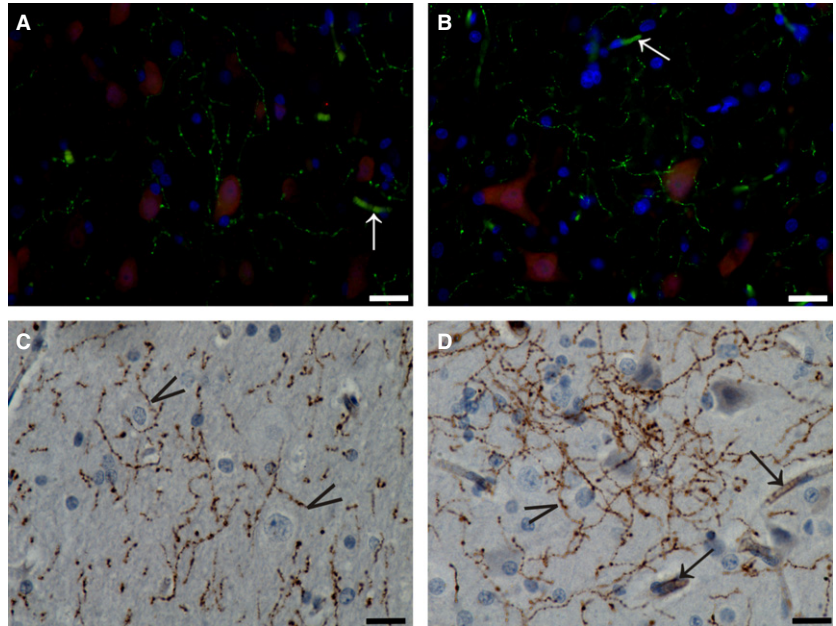


Fig. 5 TH immunostaining in the claustrum. (A, B) Immunofluorescent endothelial cells (white arrows) and axons (green) contacting cell bodies (NeuN, red). (C, D) Immunoperoxidase reaction showing TH-ir puncta and axons with varicosities running at all directions. Arrowheads indicate terminals that surrounded and defined cell bodies. Black arrows indicate positive endothelial cells. Scale bars = 10 μm.

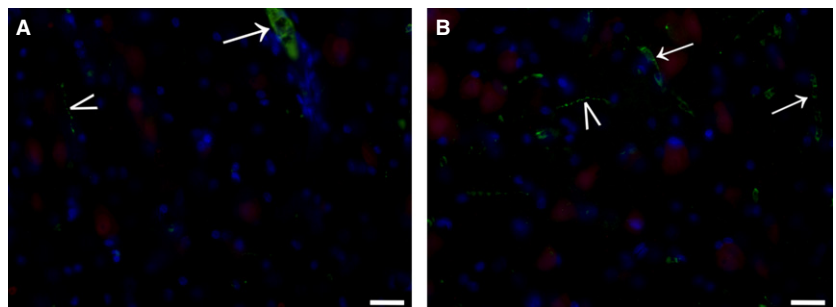


Fig. 6 DBH immunostaining in the claustrum. (A, B) Immunofluorescent (green) axons (arrowheads) and endothelial cells (arrows). Scale bars = 10 μm.

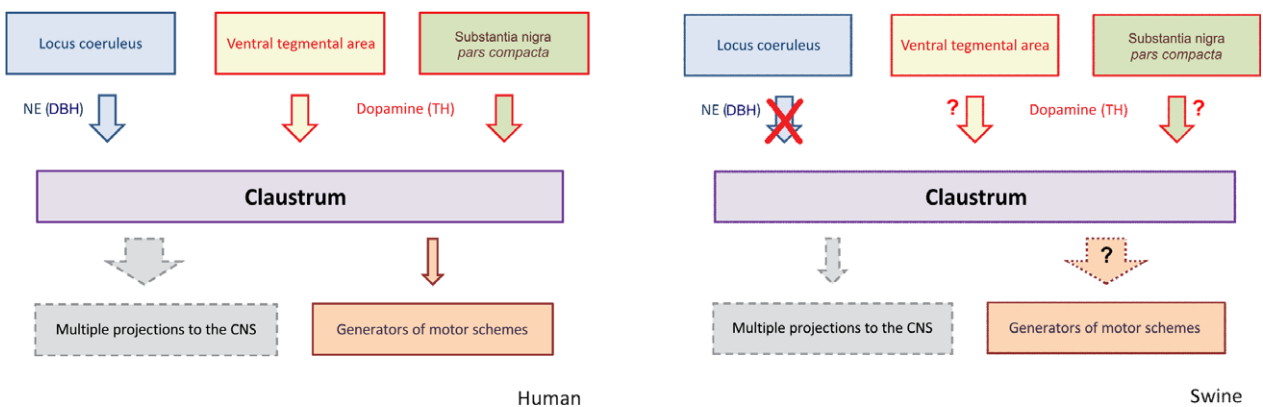


Fig. 7 Schematic representation of the possible connections between the brainstem and the claustrum in man (left) and swine (right). The top part represents the chemical pathways, and the bottom part the possible outputs.

but not TH-positive axons (Barbier et al. 2016). Dopamine, noradrenaline and serotonin were detected in the normal human CL, using high-performance liquid chromatography and electrochemical detection. Furthermore, a significant reduction of dopamine and noradrenaline content has been reported in the CL of patients affected by PD (Sitte et al. 2016).

In the past decade, several hypotheses have been proposed to associate a specific function to the CL (Crick & Koch, 2005; Smythies et al. 2012; Reser et al. 2014; Goll et al. 2015; Patru & Reser, 2015). These hypotheses share a common feature: the key factor is the reciprocal connectivity of the CL with most areas of the cerebral cortex and selected subcortical structures. Our findings hint at the possibility that brainstem catecholaminergic afferents may project to the CL. Indeed, TH-immunoreactive axons represent the dopaminergic and noradrenergic pathways from the ventral tegmental area (VTA) and the locus coeruleus, respectively (Chandler, 2016; Morales & Margolis, 2017). Dopaminergic neurons are also localized in the substantia nigra pars compacta, and their projection to the dorsal striatum constitute the nigrostriatal pathway (Ledonne & Mercuri, 2017). Thus, based on our results, CL function could be affected by direct ascending inputs from the brainstem. This latter hypothesis disagrees with the observations by Barbier et al. (2016), who did not find TH projections in the rat CL. However, in line with our hypothesis, a previous study demonstrated the presence of serotonin-containing afferents from the raphe nuclei in the CL of the crab-eating macaque *Macaca fascicularis* (Baizer, 2001). The CL of the pig seems to be reached by dopaminergic, but not noradrenergic, axons; indeed, DBH fibers were very scarce and did not contact neurons. This suggests that TH-positive innervation originates mainly from VTA or/and *substantia nigra pars compacta*, whose projections to the CL have already been reported in other species (Druga, 2014). Since TH innervation has a multiple origin, our results are not sufficient to prove an involvement of the CL in reward and motivation pathways and in the pathophysiology of PD. However, the dense dopaminergic immunoreactivity observed here supports the results of previous studies describing the pathological changes of CL in patients with PD (Braak et al. 2001, 2007; Kalaitzakis & Pearce, 2009). Furthermore, our observations provide a neuroanatomical support for a direct dopamine modulation of CL neurons, corroborating the theory proposed by Patru & Reser (2015) about their involvement in delusional states.

We would like to emphasize that our study also suggests the presence of species differences in the structures and connectivity among mammals. To a certain extent, they may simply reflect the growing complexity of the basal prosencephalon in large-brained mammals, or be indicative of a more complex connectivity spectrum in different species (Fig. 7). We also emphasize that

extrapyramidal motor pathways, and generators of motor schemes in the brainstem with all their reciprocal prosencephalic connections, have a great importance in hoofed animals, including Perissodactyla and terrestrial Cetartiodactyla (such as the pig) (for a recent description see Cozzi et al. 2017).

In conclusion, the CL of the pig is densely innervated by TH axons, which contact cell bodies within the structure, but which is scarcely innervated by DBH fibers. Such projections indicate a possible role of this nucleus in functions that are controlled by brainstem structures, and may be important in the pathophysiology of neurodegenerative pathologies, including PD.

Author contributions

A.P., V.M., B.C., E.G. conceived the study. A.P., V.M., F.C. performed the laboratory experiments. All authors analyzed the data, drafted the manuscript, revised it critically for important intellectual content, and read and approved the final manuscript.

Conflict of interest

This research was conducted in the absence of any commercial or financial relationships that could be construed as a potential conflict of interest.

References

- Baizer JS (2001) Serotonergic innervation of the primate CL. *Brain Res Bull* **55**, 431–434.
- Barbier M, Houdayer C, Franchi G, et al. (2016) Melanin-concentrating hormone axons, but not orexin or tyrosine hydroxylase axons, innervate the CL in the rat: an immunohistochemical study. *J Comp Neurol* **1498**, 1489–1498.
- Braak H, Del Tredici K, Sandmann-Kiel D, et al. (2001) Nerve cells expressing heat-shock proteins in Parkinson's disease. *Acta Neuropathol* **102**, 449–454.
- Braak H, Sastre M, Del Tredici K (2007) Development of α -synuclein immunoreactive astrocytes in the forebrain parallels stages of intraneuronal pathology in sporadic Parkinson's disease. *Acta Neuropathol* **114**, 231–241.
- Brichta L, Greengard P, Flajolet M (2013) Advances in the pharmacological treatment of Parkinson's disease: targeting neurotransmitter systems. *Trends Neurosci* **36**, 543–554.
- Cao Y, Whalen S, Huang J, et al. (2003) Asymmetry of subinsular anisotropy by in vivo diffusion tensor imaging. *Hum Brain Mapp* **20**, 82–90.
- Chandler DJ (2016) Evidence for a specialized role of the locus coeruleus noradrenergic system in cortical circuitries and behavioral operations. *Brain Res* **1641**, 197–206.
- Cortimiglia R, Infantellina F, Salerno MT, et al. (1982) Unit study in cat CL of the effects of iontophoretic neurotransmitters and correlations with the effects of activation of some afferent pathways. *Arch Int Physiol Biochim* **90**, 219–230.
- Cozzi B, Roncon G, Granato A, et al. (2014) The CL of the bottlenose dolphin *Tursiops truncatus* (Montagu 1821). *Front Syst Neurosci* **8**, 42.

- Cozzi B, De Giorgio A, Peruffo A, et al.** (2017) The laminar organization of the motor cortex in monodactylous mammals: a comparative assessment based on horse, chimpanzee, and macaque. *Brain Struct Funct* **222**, 2743–2757.
- Craine E, Daniels H** (1973) Dopamine-P-hydroxylase. *J Biol Chem* **25**, 7838–7845.
- Crick FC, Koch C** (2005) What is the function of the CL? *Philos T R Soc B* **360**, 1271–1279.
- Daubner SC, Le T, Wang S** (2012) Tyrosine hydroxylase and regulation of dopamine synthesis. *Arch Biochem Biophys* **508**, 1–12.
- Day-Brown JD, Slusarczyk AS, Zhou N, et al.** (2016) Synaptic organization of striate cortex projections in the tree shrew: a comparison of the CL and dorsal thalamus. *J Comp Neurol* **52**, 1403–1420.
- Deutch AY, Mathur BN** (2015) Editorial: the CL: charting a way forward for the brain's most mysterious nucleus. *Front Syst Neurosci* **9**, 103.
- Druga R** (2014) The structure and connections of the CL. Chapter 2. In: *The CL*. (eds Smythies J, Edelman L, Ramachandran V), pp. 29–84. Elsevier Inc.
- Edelman LR, Denaro FJ** (2004) The CL: a historical review of its anatomy, physiology, cytochemistry and functional significance. *Cell Mol Biol* **50**, 675–702.
- Fallon JH, Koziell DA, Moore RY** (1978) Catecholamine innervation of the basal forebrain. *J Comp Neurol* **180**, 545–580.
- Félix B, Léger ME, Albe-Fessard D, et al.** (1999) Stereotaxic atlas of the pig brain. *Brain Res Bull* **49**, 1–137.
- Feng Z, Angeletti RH, Levin BE, et al.** (1992) Glycosylation and membrane insertion of newly synthesized rat dopamine β -hydroxylase in a cell-free system without signal cleavage. *J Biol Chem* **267**, 21808–21815.
- Fuxe K, Agnati LF, Merlo Pich E, et al.** (1987) Evidence for a fast receptor turnover of D1 dopamine receptors in various forebrain regions of the rat. *Neurosci Lett* **81**, 183–187.
- Goll Y, Atlan G, Citri A** (2015) Attention: the CL. *Trends Neurosci* **38**, 486–495.
- Hinova-Palova DV, Edelman L, Landzhov BV, et al.** (2014) Parvalbumin-immunoreactive neurons in the human CL. *Brain Struct Funct* **219**, 1813–1830.
- Jelsing J, Hay-Schmidt A, Dyrby T, et al.** (2006) The prefrontal cortex in the Göttingen minipig brain defined by neural projection criteria and cytoarchitecture. *Brain Res Bull* **70**, 322–336.
- Johnson JI, Fenske BA, Jaswa AS, et al.** (2014) Exploitation of puddles for breakthroughs in CL research. *Front Syst Neurosci* **8**, 78.
- Kalaitzakis ME, Pearce RKB** (2009) The morbid anatomy of dementia in Parkinson's disease. *Acta Neuropathol* **118**, 587–598.
- Kowiański P, Dziewiatkowski J, Kowiańska J, et al.** (1999) Comparative anatomy of the CL in selected species: a morphometric analysis. *Brain Behav Evol* **53**, 44–54.
- Kowiański P, Dziewiatkowski J, Morys JM, et al.** (2009) Colocalization of neuropeptides with calcium-binding proteins in the claustral interneurons during postnatal development of the rat. *Brain Res Bull* **80**, 100–106.
- Ledonne A, Mercuri NB** (2017) Current concepts on the neuropathological relevance of dopaminergic receptors. *Front Cell Neurosci* **11**, 27.
- Lind NM, Moustgaard A, Jelsing J, et al.** (2007) The use of pigs in neuroscience: modeling brain disorders. *Neurosci Biobehav Rev* **31**, 728–751.
- Mathur BN** (2014) The CL in review. *Front Syst Neurosci* **8**, 48.
- Meador-Woodruff JH, Mansour A, Grandy DK, et al.** (1992) Distribution of D5 dopamine receptor mRNA in rat brain. *Neurosci Lett* **145**, 209–212.
- Morales M, Margolis EB** (2017) Ventral tegmental area: cellular heterogeneity, connectivity and behaviour. *Nat Rev Neurosci* **18**, 73–85.
- Naghavi HR, Eriksson J, Larsson A, et al.** (2007) The CL/insula region integrates conceptually related sounds and pictures. *Neurosci Lett* **422**, 77–80.
- Orman R, Kollmar R, Stewart M** (2016) CL of the short-tailed fruit bat, *Carollia perspicillata*: alignment of cellular orientation and functional connectivity. *J Comp Neurol* **1474**, 1459–1474.
- Patru MC, Reser DH** (2015) A new perspective on delusional states – evidence for CL involvement. *Front Psychiatry* **6**, 158.
- Pirone A, Cozzi B, Edelman L, et al.** (2012) Topography of Gng2- and NetrinG2-expression suggests an insular origin of the human CL. *PLoS ONE* **7**(9), e44745.
- Pirone A, Castagna M, Granato A, et al.** (2014) Expression of calcium-binding proteins and selected neuropeptides in the human, chimpanzee, and crab-eating macaque CL. *Front Syst Neurosci* **8**, 99.
- Pirone A, Magliaro C, Giannesi E, et al.** (2015) Parvalbumin expression in the CL of the adult dog. An immunohistochemical and topographical study with comparative notes on the structure of the nucleus. *J Chem Neuroanat* **64–65**, 33–42.
- Pirone A, Cantile C, Miragliotta V, et al.** (2016) Immunohistochemical distribution of the cannabinoid receptor 1 and fatty acid amide hydrolase in the dog CL. *J Chem Neuroanat* **74**, 21–27.
- Rahman FE, Baizer JS** (2007) Neurochemically defined cell types in the CL of the cat. *Brain Res* **1159**, 94–111.
- Reser DH, Richardson KE, Montibeller MO, et al.** (2014) CL projections to prefrontal cortex in the capuchin monkey (*Cebus apella*). *Front Syst Neurosci* **8**, 123.
- Reser DH, Majka P, Snell S, et al.** (2016) Topography of CL and insula projections to medial prefrontal and anterior cingulate cortex of the common marmoset (*Callithrix jacchus*). *J Comp Neurol* **525**, 1421–1441.
- Schiffmann SN, Libert F, Vassart G, et al.** (1990) A cloned G protein-coupled protein with a distribution restricted to striatal medium-sized neurons. Possible relationship with D1 dopamine receptor. *Brain Res* **519**, 333–337.
- Sitte HH, Pifl C, Rajput AH, et al.** (2016) Dopamine and norepinephrine, but not serotonin, in the human CL are greatly reduced in patients with Parkinson's disease: possible functional implications. *Eur J Neurosci* **45**, 192–197.
- Smythies J, Edelman L, Ramachandran V** (2012) Hypotheses relating to the function of the CL. *Front Integr Neurosci* **6**, 53.
- Smythies J, Edelman L, Ramachandran V** (2014) Hypotheses relating to the function of the CL II: does the CL use frequency codes? *Front Integr Neurosci* **8**, 7.
- Sorriento D, Santulli G, Del Giudice C, et al.** (2012) Endothelial cells are able to synthesize and release catecholamines both in vitro and in vivo. *Hypertension* **60**, 129–136.
- Sutoo D, Akiyama K, Yabe K, et al.** (1994) Quantitative analysis of immunohistochemical distributions of cholinergic and catecholaminergic systems in the human brain. *Neuroscience* **58**, 227–234.
- Wang Q, Ng L, Harris JA, et al.** (2016) Organization of the connections between CL and cortex in the mouse. *J Comp Neurol* **1346**, 1317–1346.

Watson GDR, Smith JB, Alloway KD (2016) Interhemispheric connections between the infralimbic and entorhinal cortices: the endopiriform nucleus has limbic connections that parallel the sensory and motor connections of the CL. *J Comp Neurol* **1380**, 1363–1380.

Supporting Information

Additional Supporting Information may be found in the online version of this article:

Fig. S1. Cryostat section of a rat brain used as positive control to verify the labeling quality of the primary antibodies. Nissl staining was performed to identify the *locus coeruleus* (LC).

Insert in the upper right corner indicates TH immunoreactivity in LC and insert in the lower right corner indicates DBH immunoreactivity in the LC. Me5, mesencephalic trigeminal nucleus; 4V, 4th ventricle.

Fig. S2. Positive neurons to DBH and TH immunoperoxidase reaction on cryostat sections of the pig brainstem at level of the locus ceruleus (black rectangles). V4, ventriculus quartus. Scale bars: (left) 500 μm , (right) 100 μm .

Fig. S3. Positive neurons to DBH and TH immunoperoxidase reaction on paraffin sections of the pig brainstem at level of the locus ceruleus (black circles). V4, ventriculus quartus. Scale bars: 500 μm .